RM L52 H21

CONFIDENTIAL

194 Copy RM L52H21

UNCLASSIELED



NACA

ECHNICAL LIBRARY

RESEARCH MEMORANDUM

INVESTIGATION OF THE VARIATION WITH REYNOLDS

NUMBER OF THE BASE, WAVE, AND SKIN-FRICTION DRAG OF

A PARABOLIC BODY OF REVOLUTION (NACA RM-10) AT MACH

NUMBERS OF 1.62, 1.93, AND 2.41 IN THE LANGLEY

9-INCH SUPERSONIC TUNNEL

By Eugene S. Love, Donald E. Coletti, and August F. Bromm, Jr.

and August F. Bromm, Jr.

Langley Aeronautical Laboratory TECHNICAL LIBRARY

Langley Field, Va.

AIRESEARCH MANUFACTURING CO. 9851-9951 SEPULVEDA BLVD. INGLEWOOD, CALIFORNIA

CLASSIFIED DOCUMENT

This material contains information affecting the National Defense of the United States within the meaning of the espionage laws, Title 18, U.S.C., Secs. 783 and 794, the transmission or revelation of which in any nanner to unauthorized person is prohibited by law.

NATIONAL ADVISORY COMMITTEE FOR AERONAUTICS

WASHINGTON

October 17, 1952

UNCLASSIFIED

CONFIDENTIAL

UNCLASSIFIED

UNCLASSIFIED

NACA RM L52H21



NATIONAL ADVISORY COMMITTEE FOR AERONAUTICS

RESEARCH MEMORANDUM

INVESTIGATION OF THE VARIATION WITH REYNOLDS

NUMBER OF THE BASE, WAVE, AND SKIN-FRICTION DRAG OF

A PARABOLIC BODY OF REVOLUTION (NACA RM-10) AT MACH

NUMBERS OF 1.62, 1.93, AND 2.41 IN THE LANGLEY

9-INCH SUPERSONIC TUNNEL

By Eugene S. Love, Donald E. Coletti, and August F. Bromm, Jr.

SUMMARY

An investigation has been made at Mach numbers of 1.62, 1.93, and 2.41 to determine the effect of varying Reynolds number upon the base, wave, and skin-friction drag of a parabolic body of revolution (NACA RM-10, no fins) for conditions of zero heat transfer. The tests covered a Reynolds number range of approximately 1×10^6 to 11×10^6 for both fixed and natural transition at each Mach number.

The results show that for laminar flow over the entire body there is a gradual increase in forebody pressure drag with increasing Reynolds number in the lower Reynolds number range; when the Reynolds number for transition is approached and exceeded, the variation is small. In general, the theories considered gave fair predictions of the forebody pressure drag. Boundary-layer transition appears to be very sensitive to surface conditions at the lowest Mach number only and flow irregularities have significant effects upon transition on the body surface and within the wake. For estimations of the skin-friction drag the Frankl-Voishel extended theory is satisfactory for the turbulent case and the incompressible Blasius theory for the laminar case; in the transition region the experimental rise was more abrupt than that predicted by any of the methods considered. Laminar-boundary-layer profiles were in good agreement with the Von Karman-Tsien profiles, and the transitional and turbulent profiles were in fair agreement with power-law profiles. Values of skin-friction drag obtained from the boundary-layer surveys were in reasonable agreement with the experimental values obtained from force and pressure measurements.





The Reynolds number of transition decreased rapidly with increasing Mach number; empirical expressions are presented that satisfy this variation. Based upon the over-all results of the investigation, an explanation is presented for the behavior of base pressure with varying Reynolds number within the Mach number range of these tests.

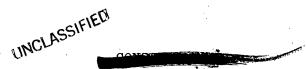
INTRODUCTION

In an effort to evaluate scale effects on slender bodies of revolution at supersonic speeds, the National Advisory Committee for Aeronautics is conducting an integrated research program at various NACA flight and wind-tunnel facilities on a slender parabolic body of revolution (with and without fins), designated as the NACA RM-10 missile. The results of several investigations undertaken as a part of this program are now available and represent a wide coverage of model scale and Reynolds number within a Mach number range from approximately 1.5 to 3.5 (refs. 1 to 10). Although the aerodynamic characteristics reported in these investigations include in some instances measurements of angle-of-attack effects, the predominant basis for correlation that appears most frequently is the drag at zero lift and the variation of the zero-lift components with Mach number and/or Reynolds number.

Thus, the purpose of the present investigation was to extend the over-all scale-effect program by measurements in the Langley 9-inch supersonic tunnel of the zero-lift drag components of a 0.0614-scale model of the RM-10 (no fins). These measurements would include the variation of base, wave, and skin-friction drag over a Reynolds number range of approximately 1×10^6 to 11×10^6 at each of three Mach numbers: 1.62, 1.93, and 2.41.

SYMBOLS

Amax	maximum cross-sectional area of body
$A_{\mathbf{w}}$	wetted area of body (surface area forward of base)
Ab	base area
$\mathtt{c}_{\mathtt{D}_{\mathtt{T}}}$	total drag coefficient, $\frac{\text{Total drag}}{q_0 A_{\text{max}}}$





 C_{D_b} base drag coefficient, $P_b(\frac{A_b}{A_{max}})$

 C_{D_F} forebody pressure-drag coefficient, $\int_0^L P_{dx}^{d} \left(\frac{r}{r_{max}}\right)^2 dx$

 $\mathbf{C}_{\mathbf{D_f}}$ average skin-friction-drag coefficient, $\mathbf{C}_{\mathbf{D_T}}$ - $\left(\mathbf{C}_{\mathbf{D_b}} + \mathbf{C}_{\mathbf{D_F}}\right)$

L body length

r local body radius

rmax maximum body radius

P pressure coefficient, $\frac{p_l - p_0}{q_0}$

P_b base pressure coefficient

 \mathbf{p}_{O} free-stream static pressure

p, local static pressure

 q_0 free-stream dynamic pressure, $\frac{\gamma}{2}p_0M_0^2$

 ${
m M}_{
m O}$ free-stream Mach number

Mach number just outside boundary layer

 U_{δ} velocity just outside boundary layer

u velocity within boundary layer

Re Reynolds number based on body length and free-stream conditions

Rem Reynolds number of transition

 $\frac{\mathbf{x}}{\mathbf{L}}$ distance from nose of model in body lengths

 γ ratio of specific heats for air (1.4)



T_e equilibrium temperature of model

To free-stream temperature

T_s free-stream stagnation temperature

 β temperature recovery factor, $\frac{T_e - T_o}{T_s - T_o}$

x coordinate in direction of body center line

APPARATUS

Wind Tunnel

The Langley 9-inch supersonic tunnel is a continuous-operation, closed-circuit type in which the pressure, temperature, and humidity of the enclosed air can be regulated. Different test Mach numbers are provided by interchangeable nozzle blocks which form test sections approximately 9 inches square. Eleven fine-mesh turbulence-damping screens are installed in the relatively large-area settling chamber ahead of the supersonic nozzle. A schlieren optical system is provided for qualitative flow observations. The turbulence level of the tunnel will be presented subsequently in comparisons to be made with other experimental results.

Models

The basic RM-10 body shape is that of a parabolic body of revolution having a tip-to-tip fineness ratio of 15. For the purpose of rocket installations in free-flight models and sting mounting of wind-tunnel models, a rearward portion of the theoretical body is removed to form a blunt-based body of fineness ratio 12.2. For this fineness ratio, the ratio of $A_{\rm W}$ to $A_{\rm max}$ is 36.38.

Two geometrically similar 0.0614-scale models were employed in the present tests. The first of these models, to be designated hereinafter as model 1, was originally intended to be used for all tests; however, as the force tests progressed the results indicated that it would be desirable to repeat these measurements with a body free of the surface fillets present on model 1. Consequently, an additional model was structed without these surface imperfections; this model is designated as model 2.

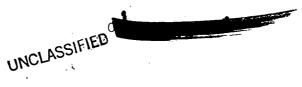


Figure 1 presents a drawing of the models showing the construction details and giving the dimensional shape equation, orifice locations (model 1 only), and body dimensions. The orifices were located along a meridian 1800 opposite from that of the assembly screws. Figure 2 presents photographs of models 1 and 2 and shows the surface coverage of the assembly-screw fillets on model 1 for the actual test condition. Model 1 was constructed of steel in essentially two meridian halves to facilitate the installation of orifice lead tubes for the pressuredistribution measurements. These lead tubes were conducted out the rear of the model within the hollow sting support. For the force tests of model 1, the lead tubes were removed and the orifice holes filled and faired with solder. For both pressure measurements and force tests the two halves of model 1 were sealed airtight. Model 2, also constructed of steel, was hollowed out for lightening purposes in two sections as shown in figure 1. These front and rear sections were permanently assembled after the internal machining and prior to profile machining to eliminate shoulder-rounding at the exterior surface juncture.

The measured ordinates of the models were within 0.001 inch of the specified values. A measurement of the surface roughness of model 1 (not to be confused with waviness) by means of a diamond-point profilometer (Physicists Research Co., model 11) indicated a surface roughness of 5 rms microinches. Though the surface roughness of model 2 was not measured, it may be assumed that its surface was equally as smooth as that of model 1, if not smoother, since more lathe polishing was devoted to its finish. It was obvious that the fillets applied to model 1 at the orifice holes and the assembly-screw positions created unavoidable local waviness in the model surface. Because of the softness of the fillet material, the surface roughness of the fillets could not be measured; however, an approximation of the waviness caused by their presence was obtained by dial depth-gage measurements. The deviation from the parabolic contour was of the order of 600 microinches to the base of the trough created by the poorest fillet.

It should be emphasized that the finish of the model surfaces was obtained through standard lathe-machining and lathe-polishing procedures and that no unusual polishing abrasives, liquid fillers, or waxes were employed. The surface roughness of the models represents, therefore, conditions which may be obtained on any model with the normal amount of care.

Balance

The balance employed in all the force tests is shown in figure 3. As shown, the balance is the free-floating sting type measuring total drag of the sting-supported model by means of a single beam equipped with strain gages. The sting shield extended just inside the model base



and its forward diameter was the same as that of the sting which supported the model during the pressure-distribution measurements, thus duplicating the geometric base conditions. The rear of the sting shield was attached by pivots to the balance box and sealed to it by means of a rubber boot cemented about the pivot point. This arrangement permitted the measured pressure within the balance box to be taken as the base pressure on the model, provided the sting shield was properly alined. The latter was assured throughout the tests by means of an electrical fouling system that operated on small tolerances.

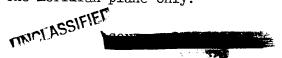
Boundary-Layer-Survey Apparatus

A drawing of the boundary-layer-survey apparatus is shown in figure 4. This apparatus is mounted on a circular metal plate which replaces one of the tunnel windows. With this plate in position, the double-wedge strut housing the traversing tube extends into the tunnel test section. The exterior traversing mechanism operates in the same manner as a standard micrometer and is graduated in thousandths of an inch. An enlarged view of the end of the total-pressure probe is shown on figure 4(b); the dimensions given were obtained from microscopic measurements.

TESTS AND PROCEDURE

All tests were conducted at Mach numbers of 1.62, 1.93, and 2.41 and over a Reynolds number range of approximately 1×10^6 to 11×10^6 at each Mach number. Throughout the tests the dew point was kept sufficiently low to insure negligible effects of condensation. A condition of zero pitch and yaw with respect to the tunnel side walls and center line, respectively, was maintained as closely as possible.

The first portion of the investigation was the measurement of the pressure distributions over model 1 along the pitch and yaw meridian planes. These meridian planes were simulated by rotating the model and sting about the center-line axis. A cathetometer was used to measure the rotation angles and to check the model yaw. A small mirror mounted in a thin sleeve installed on the sting downstream of the model base was used in conjunction with the optical angle-of-attack system to check the model pitch. Pressure distributions were obtained with the clean model and with 0.007-inch-thick (No. 180 grains) and 0.017-inch-thick (No. 60 grains) carborundum transition strips, 3/16 inch wide, as near the model nose as possible. Because of space limitations within the hollow sting, pressures over the rearmost surface of the body were obtained in separate tests and along one meridian plane only.





The second portion of the investigation was the measurement with the balance installation of the total drag and base pressure of model 1 with and without the transition strips described above. In order to check the angle of attack during these force tests a small mirror was flush-mounted in the body surface just ahead of the base. At the completion of these tests at all Mach numbers, it was concluded that premature natural transition had occurred at M=1.93. Although this pointed to some extraneous matter on the surface that was not present in the tests at the other Mach numbers, the fillets on model 1 were refaired and the force tests repeated at all Mach numbers as a check of the results. For clarity in discussions to follow, the results of the first series of force tests of model 1 will be referred to as being those for model 1-A and the results of the second series as those for model 1-B.

The third portion of the investigation was the measurement of boundary-layer profiles just ahead of the base of model 1-B.

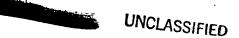
The final phase of the investigation included force measurements on a new model (model 2) to determine whether the results achieved in the tests of model 1-B approached the optimum transition Reynolds numbers for a model whose surface had no special finish but was free of surface fillets, mirror installation, and the like. In these tests, the angle of attack was checked by optical means through a window in the upper nozzle block of the tunnel.

Throughout the entire test program the models were under schlieren observation and representative schlieren photographs were taken.

REDUCTION OF DATA

All experimental pressure data have been corrected to account for the static-pressure distribution along the center line of the tunnel test section as measured in the pitch and yaw meridian planes on a long $\frac{3}{8}$ -inch-diameter cylinder having a slender ogival nose. (The mean radius of the models was 0.274 inch.) These measurements covered the range of Mach numbers and Reynolds numbers of the present tests. The buoyancy force corresponding to the correction in pressure drag has been applied to the force results. In terms of drag coefficient, the maximum buoyancy correction for any combination of Mach number and Reynolds number was about 0.01, the average correction being about 0.007 or less at M = 1.62 and 1.93, and about 0.002 at M = 2.41.

The values of stagnation temperature used to determine Reynolds number were corrected to account for the <u>difference</u> in reference bulb



temperature and the mean stagnation temperature as determined from vertical and horizontal temperature surveys within the constant-area section of the tunnel settling chamber.

The method used to reduce the boundary-layer total-pressure surveys to values of skin-friction drag was, in general, the same as that presented in reference 6. In the present case, however, the basic Crocco equation (ref. 11), which gives the temperature distribution through the boundary layer as a function of the velocity, was converted to an expression relating the Mach number to the velocity in order to facilitate the calculations. It was assumed that a condition of zero heat transfer existed for the present tests and that the Crocco relation satisfies both laminar and turbulent boundary layers provided it is modified by a reasonable temperature-recovery factor β . The Mach number-velocity relation for these conditions is

$$\frac{u}{U_8} = \frac{M}{M_8} \left(\frac{5 + \beta M_8^2}{5 + \beta M^2} \right)$$
 (1)

With this relation the compressible momentum thickness from Von Kármán's momentum integral

$$\theta_{\mathbf{c}} = \int_{0}^{\delta} \frac{\mathbf{u}}{\mathbf{U}_{\delta}} \frac{\rho}{\rho_{\delta}} \left(1 - \frac{\mathbf{u}}{\mathbf{U}_{\delta}} \right) d\mathbf{y}$$
 (2)

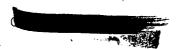
may be expressed as

$$\theta_{c} = \frac{1}{M_{\delta}^{2}} \int_{0}^{\delta} \left[MM_{\delta} \left(\frac{5 + \beta M^{2}}{5 + \beta M_{\delta}^{2}} \right)^{1/2} - M^{2} \right] dy$$
 (2a)

In like manner, equation (1) applied to the compressible displacement thickness

$$\delta_{c}^{*} = \int_{0}^{\delta} \left(1 - \frac{\rho u}{\rho_{\delta} U_{\delta}}\right) dy \tag{3}$$

UNCLASSIFIED



gives

$$\delta_{c}^{*} = \int_{0}^{\delta} \left[1 - \frac{M}{M_{\delta}} \left(\frac{5 + \beta M^{2}}{5 + \beta M_{\delta}^{2}} \right)^{1/2} \right] dy$$
 (3a)

With $\beta=1$ equations (2a) and (3a) are identical to those given in reference 12. The values of momentum and displacement thickness were calculated with $\beta=0.88$ for laminar or near-laminar boundary layers and with $\beta=1$ for turbulent boundary layers at the base. Past measurements of the equilibrium temperature of similar bodies in the 9-inch supersonic tunnel have shown values near these to exist for other bodies of revolution of similar construction.

With the values of $\theta_{\rm C}$ and $\delta_{\rm C}$ thus computed, the average skin-friction drag coefficients were obtained by the method employed in reference 6, given here as

$$C_{D_{\mathbf{f}}} = \frac{2\pi}{qA_{\max}} \left[r\rho_{\delta} U_{\delta}^{2} \theta_{\mathbf{c}} + \int_{0}^{\mathbf{x}} \rho_{\delta} U_{\delta} r \delta_{\mathbf{c}}^{*} \frac{dU_{\delta}}{d\mathbf{x}} d\mathbf{x} + \rho_{\delta} U_{\delta}^{2} \int_{0}^{\delta} \left(\frac{\rho u}{\rho_{\delta} U_{\delta}} - \frac{\rho u^{2}}{\rho_{\delta} U_{\delta}^{2}} \right) \mathbf{y} d\mathbf{y} \right]$$
(4)

PRECISION OF DATA

For all the test Mach numbers and Reynolds numbers, pressure surveys throughout the test section have shown the stream to be uniform within a maximum variation in Mach number of ±0.01. Less detailed surveys of the flow angularity have indicated negligible flow deviations; further supporting this condition are the numerous results of past investigations which have shown that zero moment and zero lift of symmetrical configurations occur, within the accuracy of the measurements, at zero angle of attack. Although the angle of attack (with respect to the tunnel side walls) could be maintained within ±0.01° of its initial setting, the accuracy of the initial alinement, approximately ±0.07°, imposed an over-all accuracy of ±0.08°. The angle of yaw (with respect to the tunnel center line) was subject to ±0.03° variation in initial reference and ±0.06° error during testing, giving an over-all accuracy





of $\pm 0.09^{\circ}$. The estimated accuracies of other test variables and the various coefficients are tabulated below:

Angle of roll, deg
Reynolds number (probable error, Re = 11×10^6) $\pm 0.04 \times 10^6$
Total drag coefficient, C_{D_T}
Forebody pressure-drag coefficient, $^{\text{C}}\mathrm{D}_{\!E}$
Base drag coefficient, C_{DB}
Average skin-friction-drag coefficient, $C_{\mathrm{D_f}}$

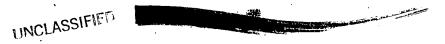
Investigations of the total-pressure probe used in the boundary-layer surveys showed that it experienced no measurable deflections in traversing the boundary layer at a given Reynolds number of the flow. Further, enlarged schlieren photographs of the boundary layer just ahead of the body base, both with and without the probe, showed no visible or measurable effect upon the condition or thickness of the boundary layer even for the case of minimum displacement thickness. From these observations and the fact that the dimensional considerations for this investigation fall within the limits of the probe-head investigations of references 12 and 13 for turbulent flow, it may be assumed that probe interference effects were small. Probe position could be measured within ±250 microinches and repeated within an estimated ±500 microinches.

RESULTS AND DISCUSSION

Pressure Distributions

The results of the pressure-distribution measurements are presented in figures 5(a), 6(a), and 7(a) for the case of natural transition. Included for comparison are the nonviscous theoretical pressure distributions given by the methods of Jones (ref. 14) and Lighthill (ref. 15). In general, both methods give fair predictions of the values and trends of the experimental results. The most noticeable discrepancy occurs near the body base where the effects of increasing Reynolds number cause decreasing pressures by eliminating the separation of the flow from the surface ahead of the base. (Additional evidence of the existence of this separation at the lower Reynolds numbers will be presented subsequently.) As shown by the experimental data, this phenomenon is common to all Mach numbers.

The results of the pressure-distribution measurements for the case of fixed transition are presented in figures 5(b), 6(b), and 7(b). The thickness of the transition strip apparently had little and no consistent





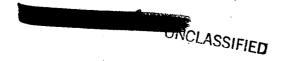
effect on the results; however, the presence of the transition strips had noticeable effects on the pressure very close to the model nose because of the expansion-shock phenomena associated with the changes in flow direction which were in turn caused by the changes in the body boundary produced by the strips. At all Mach numbers and Reynolds numbers the pressures near the base for the case of fixed transition are in general agreement with the pressures in this region for the case of natural transition at the higher Reynolds numbers where separation of the flow has been eliminated. With fixed transition, the predominant effect at all Mach numbers of an increase in Reynolds number is a slight over-all decrease in the local pressures. This effect may be explained by the fact that at the lower Reynolds numbers of the flow a large and unrealistic value of displacement thickness, as compared with that for natural transition occurring at the same body station, is realized downstream of the transition strip. As the Reynolds number of the flow is increased, a value of displacement thickness is realized which more closely duplicates the value that would be realized for turbulent flow resulting from natural transition. Thus, at the lower Reynolds numbers an abnormal radial enlargement of the profile is experienced over the entire body rearward of the transition strip that causes an increase in the body pressures.

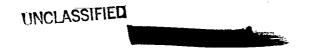
Forebody Pressure Drag

The values of forebody pressure-drag coefficient ${\rm C}_{
m DF}$ for natural and fixed transition are presented in figure 8 as a function of Reynolds number for the three Mach numbers. The local pressure coefficients used in the graphical integrations to obtain these values of ${\rm C}_{
m DF}$ were picked from a faired curve of the average of the pressure coefficients from the four meridian planes.

For natural transition there is a gradual increase in forebody pressure-drag coefficient with increasing Reynolds number in the lower Reynolds number range; at the higher Reynolds numbers the variation in ${}^{\rm C}{}^{\rm D}_{\rm F}$ is small. For fixed transition the variations are small and in most instances lie within the accuracy of the measurements with the possible exception of the results at M = 1.62 for the 0.017-inch-thick transition strip.

The variation in forebody pressure-drag coefficient with Mach number is presented in figure 9(a) for several Reynolds numbers. The non-viscous theoretical variations are also included. Here again the effect of Reynolds number is quite evident and hinders somewhat an assessment of the theoretical prediction of Mach number effects; therefore, use has been made of the boundary-layer survey results, to be discussed later,





for obtaining the value of Reynolds number at each Mach number for which the boundary-layer displacement thickness is a minimum at the body base. The values of forebody pressure-drag coefficient corresponding to the Reynolds numbers thus obtained are believed to be the values which should be used in assessing the theoretical predictions since they represent the condition for which the basic body shape is least altered by addition of the boundary layer. These values are presented in figure 9(b) and compared with the two theoretical methods considered. In general, there is fair agreement between the theories and the experimental results. Also entered on figure 9(b) are results from several other investigations. These results do not correspond to minimum boundary-layer displacement thickness at the body base; rather, they cover a wide range of Reynolds numbers and are presented to show the general correlation of results obtained in various facilities to date.

Total and Base Drag

The results of the force tests and simultaneous base pressure measurements are presented in figures 10, 11, and 12 as total drag and base drag. Discussion of these results will be in the order in which the models were tested. For all models, the ratio of sting to base diameter probably has some small effect on the values of base drag.

Model 1-A.- With the exclusion of the results at M = 1.93, the total drag for natural transition shows little variation with increasing Reynolds number until the Reynolds number is reached for which the abrupt increase in base drag is realized. Beyond this point the rise in total drag is approximately equal to the rise in base drag until the Reynolds number is approached for which the base drag is a maximum. The steady rise in total drag that takes place after the peak base drag is reached is essentially the increase in skin-friction drag resulting from the forward movement on the body surface of the region of natural transition; that is evident by comparison of the total-drag results with the forebodypressure-drag results of figure 8. Beyond its peak value, the base drag decreases and appears to approach asymptotically the base-drag values measured with fixed transition (figs. 11 and 12) which are approximately constant throughout the entire range of Reynolds number. While the thickness of the transition strip had little effect upon the base drag, the total drag shows an increase with increased thickness except at M = 1.93, for which thickness shows no measurable effect. No suitable explanation can be given for the latter except that it is possible that the thicker carborundum strip experienced flaking that reduced its effective thickness, or that the proper thicknesses were not achieved in applying the strips.

The abnormal total-drag results at M = 1.93 (fig. 11) and the accompanying change in the base drag are included to show the effects



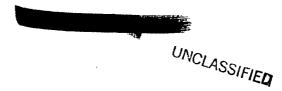


of what probably was no more than a fingerprint or an equally small accumulation of extraneous matter on the model surface since these tests were conducted between the tests at M = 2.41 and M = 1.62. Once the critical Reynolds number is reached for the surface imperfection corresponding to the presence of the extraneous matter (Re $\approx 5.5 \times 10^6$), turbulent flow is established downstream of this area. In the present case, the location and magnitude of this area and the downstream spread of turbulence caused conditions at the body base to resemble those for complete turbulent flow at the base, thereby duplicating the base drag values for fixed transition. The total drag variation beyond Re $\approx 5.5 \times 10^6$ is similar to that for fixed transition until the Reynolds number is reached for which the region of natural transition would be ahead of the area where the "triggering" matter is located. When this occurs the total drag begins to increase, as would be expected.

Model 1-B.- Although the abnormalities in total-drag and base-drag variation at M=1.93 for model 1-A did not indicate trouble with the model fillets (see fig. 2), an examination of the fillets showed that some improvement could probably be made. Therefore, all fillets were refaired and the model was tested again at all Mach numbers as model 1-B. The fixed-transition tests were not repeated. In general, excellent repetition of the drag values was obtained at all Mach numbers. At M=1.62, the only significant change was an increase in the Reynolds number for which the initial abrupt rise in base drag (and therefore, total drag) occurred from approximately 7.5×10^6 to 8.1×10^6 . This change indicated a possible increase in the Reynolds number of transition. At M=1.93, the previously mentioned abnormalities were eliminated. At M=2.41, there was little change in the results.

Model 2.- In view of the indicated possibility of an increase of transition Reynolds number for model 1-B as compared with model 1-A and in an effort to determine the effects of unavoidable fillet waviness existent on model 1-B, model 2 was tested. Only one test condition was not duplicated that had been employed in the previous tests. This was the fore and aft location of the model in the tunnel test section at M = 1.62 only. In the tests of model 1-B, schlieren observations showed that a disturbance in the tunnel test section, so weak as to be invisible at the lower Reynolds numbers, caused transition to occur prematurely on the side of the body reflecting the disturbance. (See fig. 13(a).) This phenomenon occurred only when the Reynolds number for complete transition about the periphery of the base was approached. Consequently, model 2 was shifted forward approximately 3/8 inch to allow this disturbance to clear the base. As a result, this very weak disturbance now entered the wake as shown in figure 13(b).

The results for model 2 were, in general, in excellent agreement with the results for model 1-B with the exception of the initial abrupt rise in





base drag at M = 1.62 which now occurred at Re $\approx 5.5 \times 10^6$ as against approximately 8.1×10^6 for model 1-B. This appears to be solely the result of the weak disturbance upsetting the stability of the laminar wake and thereby causing values of base drag to be increased to values corresponding to a turbulent wake. Comparison of these results for model 1-B and model 2 at M = 1.62 shows that flow irregularities and weak disturbances have a pronounced effect upon transition within the laminar wake and a lesser effect upon transition on the body surface. The significant fact to be observed here is that the base drag has been more than doubled by a phenomenon which, for a given Reynolds number, is completely independent of the condition of the boundary layer ahead of the body base, and that, while such conditions might not be encountered in flight, the possibility of their occurrence in wind-tunnel investigations calls for particular care in studies of viscous effects upon base pressure.

As shown, the results for model 2 extend to a lower Reynolds number than the results for the other models. At the lowest Reynolds number for all Mach numbers a slightly positive base pressure or thrusting force was measured. Also within the low Reynolds number range the total drag experiences a distinct rise with decreasing Reynolds number.

Boundary-Layer Surveys

The nondimensional boundary-layer profiles measured just ahead of the base of model 1-B are presented in figures 14, 15, and 16. In figure 17, the values of $\theta_{\rm C}$ used to obtain the values of $y/\theta_{\rm C}$ are presented together with the values of $\delta_{\rm C}$ as a function of Reynolds number. The laminar nondimensional profiles have been compared with the Von Karmán-Tsien compressible profiles (ref. 16) for flat plates. Freestream Mach number has been used to determine the theoretical profiles since M_{δ} is within 0.03 of the free-stream value for the cases compared and this appears to be within the assumptions of the theory. The typical Blasius (M = 0) profile has also been included in the left-hand profile of each figure to show both the experimental and theoretical effect of compressibility. (The Blasius profile is known to be correct at low to moderate subsonic speeds.)

At all Mach numbers the Von Kármán-Tsien profiles are in good agreement with the experimental values with the exception of the values at the lowest Reynolds numbers where a separation profile is shown by the experimental values. The inadequacy of the Blasius profile is clearly shown in every case.

The transitional and turbulent profiles have been compared with the power-law profile which appeared to fit best the experimental results. In agreement with what is known to occur for subsonic flow, the profiles





progress in shape in decreasing power values of the power-law profile. Though the Reynolds number range of the present tests was only adequate enough to approach a $\frac{1}{7}$ -power profile, reference 9 has shown that at higher Reynolds numbers a $\frac{1}{7}$ -power profile gives good agreement with the experimental profile.

In figure 17, the values of Reynolds number of transition at the body base determined from schlieren photographs are compared with the region of change from negative to positive slope of the faired curves of the variation of $\delta_{\rm C}$ and $\theta_{\rm C}$ with Reynolds number. There is obviously some room for choice in the fairing of the curves in this region and the comparison is limited accordingly. The values indicated for the schlieren observations were determined from enlarged schlieren photographs in a manner similar to that employed in reference 17. In the present case the values of Reynolds number of transition were determined by extrapolating to zero distance from the base the curves showing the variation with Reynolds number of the observed beginning of transition in terms of distance from the body base. As shown in figure 17, the values of Reynolds number of transition thus obtained are in good agreement with the results obtained from the boundary-layer surveys.

Skin-Friction Drag

The values of skin-friction-drag coefficient determined from the force and pressure measurements and from the boundary-layer surveys are presented in figures 18, 19, and 20. For comparison with the experimental results for fixed transition, three methods for predicting the turbulent skin-friction drag were used. The first of these was the semiempirical relation for incompressible flow for Reynolds numbers less than 10^7 :

$$c_f = 0.074(Re)^{-1/5}$$
 (5)

The second was the Frankl-Voishel extended theory of reference 12 which was shown to give good agreement with flat-plate experimental results at M=2.5. For the present case the expression was adapted to equation (5) which gives

$$c_f = 0.074 (Re)^{-1/5} \left(\frac{1}{1 + \frac{\gamma - 1}{2} M_0^2} \right)^{0.467}$$
 (6)



UNCLASSIFIED



The third method was the Von Kármán estimation of reference 18 applied to equation (5). This method and that of equation (5) are believed to represent the lower and upper extremes, respectively, of available theories.

For comparison with the experimental results for laminar flow over the entire body, three methods for predicting laminar skin-friction drag were used. The first of these was the incompressible Blasius relation (with the Topfer constant)

$$c_f = \frac{1.328}{\sqrt{\text{Re}}} \tag{7}$$

The second was the method of Von Karman and Tsien expressed here as

$$c_{f} = \frac{K}{\sqrt{Re}}$$
 (8)

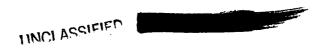
where K is a function of M_0 and is given in reference 16. The third method was that of Chapman and Rubesin. This relation is

$$c_{f} = \frac{1.328}{\sqrt{\text{Re}}\sqrt{C}} \tag{9}$$

where the constant C is dependent upon Mach number and is determined as shown in reference 19.

All of the above predictions for both laminar and turbulent skin friction are for flat plates with zero pressure gradient and zero heat transfer. Mangler (ref. 20) has given a method for transforming laminar skin-friction values for a flat plate to those for bodies of revolution having an analogous pressure distribution. Also, an approximation was given for transforming turbulent flat-plate values. The constants for the Mangler transformation that correspond to the cut-off RM-10 body have been calculated and are 1.06 for the laminar case and 1.014 for the turbulent case. Curves of the three laminar theories modified by the appropriate Mangler constant have been included in figures 18, 19, and 20 along with the unmodified curves. No such inclusion has been made for the turbulent predictions because of the insignificant change indicated.

For comparison with the experimental trends of the so-called transition curves, three methods were employed. The first of these was the



17

flat-plate incompressible approach given in reference 21

$$c_{f} = \left(1 - \frac{Re_{T}}{Re}\right) \frac{A}{\left(Re - Re_{T}\right)^{1/5}}$$
 (10)

with A = 0.074. The second used the relation of equation (10) but with the value of A determined by the Monaghan relation (ref. 22)

$$A = 0.074 \left[1 + 0.176 M_0^2 \right]^{-0.44}$$
 (11)

which was shown to give good agreement with results of several supersonic investigations. (A relation identical with eq. (11) except for a value of -0.348 for the exponent has been suggested in ref. 23 and shown to give good agreement with experimental results at the extremities of the transition curve for a flat plate at $M_0 \approx 2.2$.) The third method employed was the flat-plate incompressible relation

$$c_f = 0.074(R_e)^{-1/5} - \frac{N}{Re}$$
 (12)

where the value of constant N was determined by the same approach required for use of equation (10). (See refs. 21 and 23.)

The experimental results from the force and pressure measurements show scatter that, for a given model, is within the experimental accuracy. The small difference between the results for different models, particularly between model 1-B and model 2, is encouraging since it shows that the profile and surface roughness of small models may be duplicated through normal machining processes to a degree satisfactory for determining the effects upon skin friction of such variables as body shape and other parameters. The general agreement of the values obtained from the boundary-layer surveys with the other experimental values for model 1-B is also within the combined accuracy of the two experimental methods. This is particularly significant in that it shows that the single-probe survey method gives reasonable results even for the conditions for which the boundary layer was very thin (that is, ratio of probe height to boundary thickness of the order of 1/3) and therefore more subject to interference effects.

Comparisons of the experimental results and the various theoretical estimates indicate several conclusions. For the case of fixed transition, and therefore turbulent flow over all the body except the very tip, the Frankl-Voishel extended theory for a flat plate gives a reasonable





prediction of the turbulent skin friction. For the case of laminar flow over the entire body, there is a general agreement between the experimental results and most of the laminar predictions; this general agreement results from a combination of the experimental accuracy and the small differences between the theoretical curves. assessment of the value of the Mangler transformation or the relative merits of the flat-plate theories is impossible. It does seem permissible, however, to draw the same conclusion here that has been reached in reference 24 for cone-cylinder bodies of revolution, namely, that the simple Blasius incompressible theory for a flat plate gives a satisfactory prediction. (This conclusion is not intended to violate the fact that the measured laminar boundary-layer profiles were in close agreement with the Von Karman-Tsien profiles. The more recent work of Young and Janssen (ref. 25) conclusively supports the Von Karmán-Tsien predictions that for a given value of $\,u/U_{\delta}\,$ an increase in Mach number can only increase the value of y/θ_c .) At M = 2.41, all of the experimental results indicate a more rapid decrease in laminar skin friction with increasing Reynolds number than predicted by the theories.

The method that gives a transition curve which appears to be in best agreement with the experimental results is that given by equation (10) with the incompressible value of A = 0.074 (see letter K on figures); however, as the completely turbulent condition is approached, this method will be inadequate since the flat-plate turbulent incompressible theory is inadequate. In addition, the experimental transition results show a more abrupt rise than that predicted by any of the methods. This abrupt rise was also observed for the cone-cylinder bodies of reference 24.

Comparison of Present Results With Those Obtained

in Langley 4- by 4-Foot Supersonic Tunnel

The results of the investigation of reference 9 conducted in the Langley 4- by 4-foot supersonic tunnel at a Mach number of 1.6 (mean value = 1.61) afford an almost ideal scale-effect comparison with the present results at M = 1.62. The model length of 50 inches for the former tests compared to 9 inches for the present tests gives a geometric scale factor of 5.556 which for the present comparison also indicates the scale factor applicable to the Reynolds number of the flow for the two facilities, since the Mach number difference is small and the stagnation temperatures of the two facilities were of the same order. Moreover, the surface roughness of the models and the static-pressure and Mach number variations within the test sections of the two tunnels were of the same order.

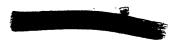




In figures 21(a) and 21(b) are presented the results of turbulence level measurements (horizontal velocity component only) made in the entrance cone of the 9-inch supersonic tunnel in conjunction with the present tests. Horizontal surveys were made along the center of the tunnel and 6 inches above the center from the vertical center plane to the west wall. At the station of measurement the local velocity was approximately 180 feet per second and the width of the tunnel was 8.75 inches, the same as for the test section. (Test section Mach number was 1.93.) The surveys show the turbulence level to remain essentially constant at a given total pressure until about 1 inch from the wall where the turbulence level begins to rise. Also indicated is the increase of turbulence level with total pressure. Figure 21(c) presents a comparison of the present turbulence level measurements in the entrance cone and those measured in the test section at M = 1.93 several years previously. The frequency sensitivity of the equipment employed in the test-section measurements was relatively low for the speeds encountered; therefore, the accuracy of these measurements is lower than that for the entrance cone measurements and the comparison can be considered firstorder only. Indications are that the turbulence level in the test section is of the same order as that in the entrance cone.

Figure 21(d) presents the variation with total pressure of the turbulence level in the entrance cone together with similar measurements made with the same equipment in the entrance cone of Langley 4- by 4-foot supersonic tunnel at a station having a local velocity of 155 feet per second. The values measured on the center line in the present tests at stagnation pressures of 90 and 120 inches of mercury absolute may be higher than those shown, since, for these two points only, insufficient experimental data prevented accurate extrapolations of the probe calibration constant. All the data at 6 inches above the center line may be considered reliable. The increase of turbulence level with stagnation pressure is clearly shown. The importance, therefore, of weighting the turbulence level against the scale of the flow (Reynolds number per unit of length) in comparisons of experimental results between different facilities seems justified. Without this weighting, the sufficiency of the Reynolds analogy remains in question. Comparison of the results for the two tunnels indicates, within the limitations of the small amount of experimental data, that for a given Reynolds number of the flow the turbulence level in the entrance cone of the 4- by 4-foot supersonic tunnel is roughly 3 to 4 times that measured in the entrance cone of the 9-inch supersonic tunnel.

A comparison of the experimental results for total drag for natural and fixed transition and for base drag from the two test facilities is presented in figure 10. The base drag curve from reference 9 has been refaired in the Reynolds number range of 8×10^6 to 11×10^6 to pass through the experimental points since the trend indicated by the experimental points corresponds to that which has recently been found to exist





generally for slender parabolic bodies. As shown in figure 10 the agreement in the trend of the total and base drag curves for the two investigations is good. In the case of the total drag for both natural and fixed transition, the curves of reference 9 give lower drag and, with respect to the present results, appear to be translated to the right by an increment of 1×10^6 to 2×10^6 in Reynolds number. The abrupt rise in the total drag, resulting from the abrupt increase in base drag. appears to occur somewhat prematurely in view of the higher transition Reynolds number indicated for the results of reference 9, and may be caused either by a phenomenon similar to that previously discussed and shown to cause the earlier rise in base drag for model 2 in the present tests or possibly by the marginal value of the ratio of sting length to base diameter. Neglecting the effect of the indicated higher Reynolds number of transition for the results of reference 9, the magnitudes of the base-drag results for the two investigations are in good agreement. No suitable explanation has been found for the differences in magnitude of the total-drag results.

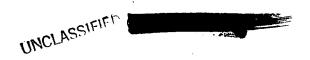
The boundary-layer-profile results for the two investigations have been compared in figure 14, second profile from the left. The Reynolds number for the present tests is 6.35×10^6 while that for the profile from reference 9 is 6.4×10^6 . The agreement between the two experimental profiles is poor. The profile of reference 9 lies well below the present results and, in contrast to the predicted Mach number effects of references 16 and 25, even below the Blasius (M = 0) profile. This discrepancy cannot be considered too important, however, since, as stated in reference 9, the results of the boundary-layer surveys may be somewhat questionable.

Entered in figure 18 is the faired experimental transition curve for skin-friction drag obtained from reference 9. The indicated higher Reynolds number of transition for the results of reference 9 is clearly shown. Although not included in figure 18, comparison of the skin-friction-drag values in the laminar range showed, in general, good agreement.

Effect of Mach Number Upon Reynolds

Number of Transition

The Reynolds number of transition is defined here as the Reynolds number for which the abrupt rise in skin-friction drag takes place. The values of these Reynolds numbers were selected from the experimental results of figures 18, 19, and 20 and are tabulated on the following page.



UNCIASSIFIED 21

The value for model 1-A at M = 1.93 has been omitted since it represents conditions other than those for natural transition:

Model	Reynolds number of transition at -		
	M = 1.62	M = 1.93	M = 2.41
1-A	8.4 × 10 ⁶	~ ~ = = = = = = = =	6.0 × 10 ⁶
1-B	8.8	7.5 × 10 ⁶	6.0
2	9.2	7.5	6.0

The successive improvements to the model surface condition represented by the different models are seen to have had little effect upon the transition at M = 1.93 and 2.41. However, at M = 1.62 the Reynolds number of transition was increased almost 1×10^6 . Apparently at the lower Mach number, transition is more sensitive to surface condition.

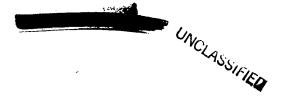
From figure 22, the effect of increasing Mach number in decreasing the Reynolds number of transition for the RM-10 body is seen to be appreciable. This effect, while in opposition to the conclusion drawn in reference 26, is in agreement with the theoretical predictions of references 27 and 28 for the case of zero heat transfer and with the experimental findings for the cone-cylinder bodies of revolution investigated in reference 24. (The data of ref. 26 are believed to be insufficiently screened to assess the case of zero heat transfer.)

A purely empirical relation has been fitted to the present results for model 2 and a relation between the Mach number and Reynolds number that gives excellent agreement is found to be

$$Re_{\rm T} = \frac{17.8 \times 10^6}{M_0^{5/4}} \tag{13}$$

In reference 24 the relation

$$Re_{T} = \frac{23 \times 10^{6}}{M_{0}^{2} - 1} \tag{14}$$



was found to be in good agreement with the experimental results for cone-cylinder bodies; however, the lowest Mach number of this investigation was M = 2.45. As the Mach number is decreased from a value of 2, this relation (eq. (14)) would be expected to become increasingly inadequate since at M_0 = 1, Re_T becomes infinite. In contrast, at M_0 = 1, equation (13) gives a value of 17.8 × 10⁶ which, omitting such phenomena as shock-boundary layer interactions common to transonic flow, seems realistic in view of values of Re_T in excess of 17.8 × 10⁶ that have been measured in subsonic flow. A relation that gives a reasonable prediction of the experimental results for the cone-cylinder bodies of reference 24 and also for other results for cone-cylinder and ogive-cylinder bodies at lower Mach numbers is

$$Re_{T} = \frac{15 \times 10^{6}}{\left(M_{O} - 1.75\right)^{2} + 3} \tag{15}$$

The curves given by equations (13), (14), and (15) are presented in figure 22 together with the related experimental data. In all cases the surface roughness of the models was of the same order and the test conditions were stable for zero heat transfer. The variation in Reynolds number for the results of reference 24 was achieved by lengthening the model in contrast to a variation obtained by increasing density for the other results. In addition, some of the experimental results of reference 24 were obtained from base-pressure curves, which, as will be shown subsequently, is apparently a satisfactory method.

Whether or not equation (13) for the RM-10 body is satisfactory beyond the range of the present tests will, of course, remain a question until additional, properly screened, experimental data are obtained. same applies to equation (15). Insofar as the RM-10 body is concerned, figure 23, which gives the magnitude of the pressure gradient at the rear of the body as a function of Mach number, indicates that there should be a decrease in the adverse pressure gradient at the body base with increasing Mach number. The fact that this adverse pressure gradient occurs gradually and near the base for the RM-10 body may explain the higher values of Rem for this body as compared with the cone-cylinder bodies for which the adverse pressure gradient occurs abruptly and immediately behind the cone-cylinder juncture. The interrelationship between Mach number and the severity of the adverse pressure gradients gives reason to suspect that both equations (13) and (15) may predict too large a value of Rem in the low supersonic Mach number range, particularly so for equation (15) in its application to cone-cylinder bodies.



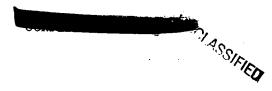


Results and Correlation of Schlieren Observations

Figure 24 presents two schlieren photographs of model 1-B at M=1.93 taken in rapid succession at a Reynolds number of 7.55×10^6 . The upper photograph shows a turbulence burst occurring on the body surface while the lower, which agreed with two other photographs taken at the same time, shows no such phenomenon. The results of figure 19 indicate that this turbulence burst is occurring near the Reynolds number corresponding to that for initial transition.

Figure 25 presents several schlieren photographs of model 1-B at M = 1.62 and shows the effect of increasing Reynolds number upon the trailing shock and boundary-layer phenomena. For these photographs the model was supported by the sting used in the pressure-distribution tests but without the mirror sleeve. At a Reynolds number of 3.18×10^6 the laminar flow apparently separates slightly from the body surface ahead of the base as indicated by the profiles of figure 14. The boundary of the laminar wake experiences no perceptible change in direction at the body base, but progresses downstream in a continuing convergent pattern until it is deflected by the sting's presence. The point of this deflection establishes the location of the trailing shock. As the Reynolds number is increased to 6.29×10^6 , the apparent separation ahead of the base appears to be almost completely eliminated. The boundary of the laminar wake still leaves the body base smoothly and continues its convergent pattern. The location of the trailing shock has now moved slightly upstream with the increase in Reynolds number.

At a Reynolds number of 8.07×10^6 the trailing shock was observed to oscillate fore and aft erratically, its rearmost movement being slightly ahead of that for Re = 6.29×10^6 . Several schlieren photographs were taken of this phenomenon, two of which are presented here. In one, the trailing shock was caught in the midst of an oscillation in the upstream direction. In this photograph, the peculiarity about the trailing shock is that the inner portion appears to be broken or separated from the outer portion, the inner portion being farther upstream. The other photograph at Re = 8.07×10^6 shows an unbroken trailing shock lying approximately at the most forward position of oscillation. The significance of the broken-shock phenomenon is believed to lie in its association with turbulent wakes. Shadowgraphs of projectiles in flight made by the Ballistic Research Laboratories, some of which are presented in reference 29, show that broken-shock phenomena arise from turbulent wakes only. (This does not imply that the phenomenon is a necessary condition for turbulent wake.) Further evidence of this relation is given by the excellent correlation between the value of Reynolds number for the abrupt rise in base drag for this model (Re = 8.05×10^6 .



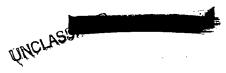
from fig. 10) and the Reynolds number at which this shock phenomenon occurs (Re = 8.07×10^6). This abrupt rise in base drag could only be achieved by a sudden increase in scavenging common to turbulent flow, thus indicating that transition has occurred in the wake close to the body base. Of particular importance is the fact that this transition takes place within the wake and not on the body surface ahead of the base. Figures 10, 18, and the schlieren photographs at Re = 8.07×10^6 and 8.28×10^6 show that laminar flow still exists on the body surface ahead of the base.

The schlieren photographs at Reynolds numbers of 9.61×10^6 and 10.77×10^6 show that transition has occurred on the body surface and that the region of transition is moving forward with increasing Reynolds number.

The above explanations of the abrupt rise in base drag would also seem to support the belief mentioned previously that the premature rise in the base drag of model 2 at M=1.62 is a result of the weak disturbance being allowed to intersect the laminar wake, thereby triggering wake transition.

Observations on the General Base-Pressure Phenomena

Consideration of the results of this investigations leads to a general insight into the observed behavior of base pressure with varying Reynolds number within the Mach number range of these tests. At low Reynolds numbers a laminar wake enshrouds the base area and, as a result of the low viscous scavenging, the base pressure is relatively high, even positive at very low Reynolds numbers. So long as the wake remains laminar, the base pressure should decrease only slightly with increasing Reynolds number, since for laminar flow the viscous scavenging increases very gradually with increasing Reynolds number. At some point the Reynolds number will be reached for which the free laminar wake can no longer maintain its stability. When this Reynolds number is reached, transition to turbulent flow will occur in the wake. The point in the wake at which this transition occurs will initially move forward very rapidly with increasing Reynolds number, but as this point approaches closely the edge of the body base its forward travel will become considerably slower. Now, the base pressure decreases according to the increase in scavenging, which is directly related to the rate at which the wake progresses from fully laminar to fully turbulent. Therefore, there will initially be an abrupt decrease in base pressure followed by a slowing-down of the rate of decrease. The base pressure will continue to decrease very slowly with increasing Reynolds number, since, though most of the base area is subjected to the scavenging of a turbulent wake, there remains a small length of free laminar wake just aft of the edge of



the body base in which the initial point of turbulence moves forward very slowly toward the body. Thus, when this point reaches the edge of the body base, the entire wake will be fully turbulent and a near minimum in base pressure has been reached without transition on the body.

The term "near minimum" has been employed since there appears to be one other condition that can cause a small further decrease in base pressure. When the Reynolds number has been reached for which the entire wake is turbulent, the Reynolds number for transition on the body surface just ahead of the base has been closely approached. For the latter condition, the momentum thickness of the boundary layer has ceased to have a rate of decrease that is essentially proportional to the rate of decrease of the displacement thickness, but remains almost constant while the displacement thickness continues its decrease. This is true for natural transition in general as indicated by the decrease in the boundary-

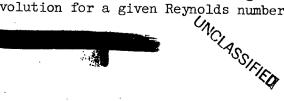
layer form parameter $H = \frac{\delta_c^*}{\theta_c}$ as transition is approached. The result

is that a small additional decrease in base pressure is realized. Thus, a well-defined minimum decrease in base pressure corresponds to the Reynolds number just prior to that for which fully turbulent flow first appears on the body surface ahead of the base. The degree to which this small additional decrease in base pressure will make itself felt will be dependent primarily upon the ratio of boundary-layer thickness to base diameter and, secondarily, upon boattail angle. If the former is sufficiently small, the additional decrease in base pressure will be insignificant, and there will be no well-defined minimum base pressure.

With an increase in Reynolds number beyond that for transition on the body surface, the displacement and momentum thickness increase almost proportionately until turbulent flow is realized over the entire body. Accordingly, the base pressure increases slightly, tending to become asymptotic to the value corresponding to turbulent flow over the entire body.

From the above analogy, the Reynolds number corresponding to the minimum base pressure (maximum peaks in base drag) may be assumed to give a satisfactory indication of the Reynolds number for which transition first takes place on the body surface. This correlation of Reynolds number of transition on the body surface and of minimum base pressure should also apply, within the Mach number range of the present investigations, to all body shapes. For bodies showing no well-defined minimum base pressure, but rather a minimum which appears to cover an appreciable Reynolds number range, the Reynolds number of transition on the body surface would correspond to the value of minimum base pressure at the start of its last gradual increase.

At the present time, a theoretical prediction of the magnitude of base pressure on bodies of revolution for a given Reynolds number, Mach





number, and body shape seems almost an impossibility. The problem of wake stability cannot be neglected, and the interdependence of Reynolds number of transition on the body surface, Mach number, pressure gradients, and body shape, and the Reynolds number of transition (or stability) of the free wake must be reckoned with even for the case of zero heat transfer.

CONCLUSIONS

An investigation has been conducted in the Langley 9-inch supersonic tunnel to determine the effect of varying Reynolds number upon the base, wave, and skin-friction drag of a parabolic body of revolution (NACA RM-10, no fins) at zero lift and for zero heat transfer. The tests covered a Reynolds number range of approximately 1×10^6 to 11×10^6 for both fixed and natural transition at each of three Mach numbers: 1.62, 1.93, and 2.41. The following conclusions are indicated:

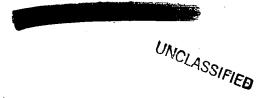
- 1. For natural transition there is a gradual increase in forebody pressure drag with increasing Reynolds number. This increase becomes less as the Reynolds number of transition is approached. Beyond the Reynolds number of transition, the variation in forebody pressure drag is small. For transition fixed near the body nose, the variation in forebody pressure drag is small over the entire Reynolds number range.
- 2. The variation in forebody pressure drag with Mach number is dependent upon the Reynolds number considered. The methods of Jones and Lighthill give a fair prediction of the experimental results for the Mach number range of these tests.
- 3. Boundary-layer transition appears to be more sensitive to surface conditions at the lowest Mach number. Flow irregularities and weak disturbances have a pronounced effect upon transition within the laminar wake and a lesser, though significant, effect upon transition on the body surface.
- 4. Results of turbulence-level measurements made in the entrance cone of the tunnel in conjunction with the present tests indicate a low turbulence level and an increase in turbulence with increasing Reynolds number of the flow. Comparison of these results with results of measurements made several years previously in the test section at M=1.93 gives an indication, which can be considered first-order only, that the turbulence level experiences little change in passing from subsonic to supersonic flow when the subsonic turbulence level is relatively low.
- 5. At all Mach numbers, the Frankl-Voishel extended theory gives a reasonable prediction of the turbulent skin-friction drag (with transition fixed near the body nose), and the Blasius incompressible theory

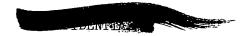


gives a satisfactory prediction of the laminar skin-friction drag. The rise in skin-friction drag in the transition region is slightly more abrupt than the best prediction of the methods considered.

- 6. Boundary-layer profiles for laminar flow show good agreement with the compressible profiles of Von Kármán and Tsien at all Mach numbers. The transitional and turbulent profiles are in fair agreement with decreasing power-law profiles with increasing Reynolds number. Skin-friction-drag coefficients determined from the boundary-layer surveys are in reasonable agreement with those obtained from the force and pressure measurements.
- 7. The Reynolds number of transition decreases rapidly with increasing Mach number. Empirical relations are presented that show good agreement with the experimental results of this investigation and with results for cone-cylinder and ogive-cylinder bodies from other investigations.
- 8. Based upon schlieren observations and the over-all results of this investigation, an explanation is presented for the behavior of base pressure with varying Reynolds number that should apply to slender bodies of revolution in general within the Mach number range of these tests. When the flow over the entire body is laminar, wake stability is shown to be the primary influencing variable upon base pressure.

Langley Aeronautical Laboratory,
National Advisory Committee for Aeronautics,
Langley Field, Va.

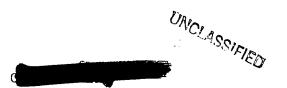




REFERENCES

- 1. Luidens, Roger W. and Simon, Paul C.: Aerodynamic Characteristics of NACA RM-10 Missile in 8- by 6-Foot Supersonic Wind Tunnel at Mach Numbers From 1.49 to 1.98. I Presentation and Analysis of Pressure Measurements (Stabilizing Fins Removed). NACA RM E50Dl0, 1950.
- 2. Esenwein, Fred T., Obery, Leonard J., and Schueller, Carl F.: Aero-dynamic Characteristics of NACA RM-10 Missile in 8- by 6-Foot Supersonic Wind Tunnel at Mach Numbers From 1.49 to 1.98.
 II Presentation and Analysis of Force Measurements. NACA RM E50D28, 1950.
- 3. Luidens, Roger W., and Simon, Paul C.: Aerodynamic Characteristics of NACA RM-10 Missile in 8- by 6-Foot Supersonic Wind Tunnel at Mach Numbers From 1.49 to 1.98. III Analysis of Force Distribution at Angle of Attack (Stabilizing Fins Removed). NACA RM E50119, 1950.
- 4. Chauvin, Leo T. and deMoraes, Carlos A.: Correlation of Supersonic Connective Heat-Transfer Coefficients From Measurements of the Skin Temperature of a Parabolic Body of Revolution (NACA RM-10). NACA RM L51A18, 1951.
- 5. Jackson, H. Herbert, Rumsey, Charles B., and Chauvin, Leo T.: Flight Measurements of Drag and Base Pressure of a Fin-Stabilized Parabolic Body of Revolution (NACA RM-10) at Different Reynolds Numbers and at Mach Numbers From 0.9 to 3.3. NACA RM L50G24, 1950.
- 6. Rumsey, Charles B. and Loposer, J. Dan: Average Skin-Friction Coefficients From Boundary-Layer Measurements in Flight on a Parabolic Body of Revolution (NACA RM-10) at Supersonic Speeds and at Large Reynolds Numbers. NACA RM L51B12, 1951.
- 7. Perkins, Edward W., Gowen, Forrest E., and Jorgensen, Leland H.:
 Aerodynamic Characteristics of the NACA RM-10 Research Missile in
 the Ames 1- by 3-Foot Supersonic Wind Tunnel No. 2 Pressure and
 Force Measurements at Mach. Numbers of 1.52 and 1.98. NACA
 RM A51G13, 1951.
- 8. Hasel, Lowell E., Sinclair, Archibald R., and Hamilton, Clyde V.:
 Preliminary Investigation of the Drag Characteristics of the
 NACA RM-10 Missile at Mach Numbers of 1.40 and 1.59 in the Langley
 4- by 4-Foot Supersonic Tunnel. NACA RM L52A14, 1952.





- 9. Czarnecki, K. R., and Marte, Jack E.: Skin-Friction Drag and Boundary-Layer Transition on a Parabolic Body of Revolution (NACA RM-10) at a Mach Number of 1.6 in the Langley 4- by 4-Foot Supersonic Pressure Tunnel. NACA RM L52C24, 1952.
- 10. Czarnecki, K. R., and Sinclair, Archibald R.: Preliminary Investigation of the Effects of Heat Transfer on Boundary-Layer Transition on a Parabolic Body of Revolution (NACA RM-10) at a Mach Number of 1.61. NACA RM L52E29a, 1952.
- ll. Crocco, Luigi: Transmission of Heat From a Flat Plate to a Fluid Flowing at a High Velocity. NACA TM 690, 1932.
- 12. Rubesin, Morris W., Maydew, Randall C., and Varga, Steven A.: An Analytical and Experimental Investigation of the Skin Friction of the Turbulent Boundary Layer on a Flat Plate at Supersonic Speeds. NACA TN 2305, 1951.
- 13. Wilson, R. E., and Young, E. C.: Aerodynamic Interference of Pitot Tubes in a Turbulent Boundary Layer at Supersonic Speed. CF 1351 (UT/DRL 228), Contract NOrd-9195, Bur. Ord., Univ. Texas, Defense Res. Lab., Dec. 6, 1949.
- 14. Jones, Robert T., and Margolis, Kenneth: Flow Over a Slender Body of Revolution at Supersonic Velocities. NACA TN 1081, 1946.
- 15. Lighthill, M. J.: Supersonic Flow Past Bodies of Revolution. R. & M. No. 2003, British A.R.C., 1945.
- 16. Von Karman, Th., and Tsien, H. S.: Boundary Layer in Compressible Fluids. Jour. Aero. Sci., vol. 5, no. 6, Apr. 1938, pp. 227-232.
- 17. Jack, John R., and Burgess, Warren C.: Aerodynamics of Slender Bodies at Mach Number of 3.12 and Reynolds Numbers From 2×10^6 to 15×10^6 . I Body of Revolution With Near-Parabolic Forebody and Cylindrical Afterbody. NACA RM E51H13, 1951.
- 18. Von Kármán, Th.: The Problem of Resistance in Compressible Fluids. R. Accad. d'Italia, Cl. Sci. Fis., Mat. e Nat., vol. XIV, 1936. (Fifth Volta Congress held in Rome, Sept. 30 Oct. 6, 1935.)
- 19. Chapman, Dean R., and Rubesin, Morris W.: Temperature and Velocity Profiles in the Compressible Laminar Boundary Layer With Arbitrary Distribution of Surface Temperature. Jour. Aero. Sci., vol. 16, no. 9, Sept. 1949, pp. 547-565.

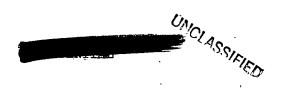


UNCLASSIFIED

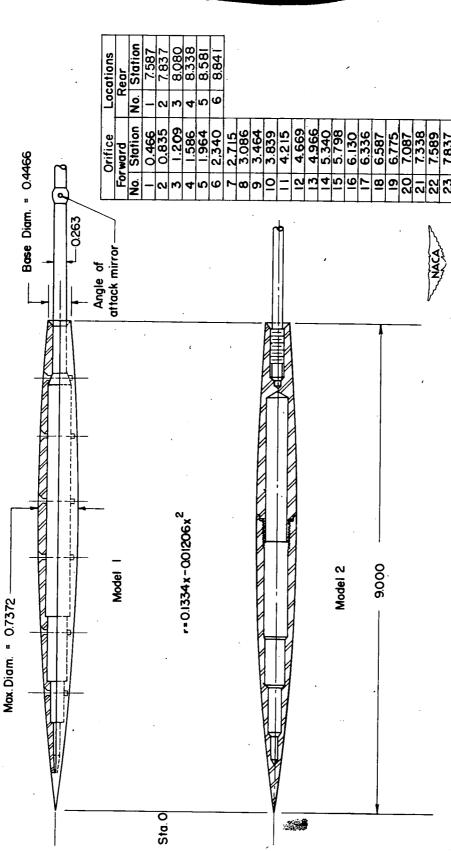


- 20. Mangler, W.: Boundary Layers With Symmetrical Airflow About Bodies of Revolution. Rep. No. R-30-18, Part 20, Goodyear Aircraft Corp., Mar. 6, 1946.
- 21. Prandtl, L.: The Mechanics of Viscous Fluids. Vol. III of Aerodynamic Theory, div. G, W. F. Durand ed., Julius Springer (Berlin), 1935, pp. 56-62.
- 22. Monaghan, R. J.: Comparison Between Experimental Measurements and a Suggested Formula for the Variation of Turbulent Skin-Friction in Compressible Flow. TN No. Aero 2037, British R.A.E., Feb. 1950.
- 23. Wilson, R. E., Young, E. C., and Thompson, M. J.: 2nd Interim Report on Experimentally Determined Turbulent Boundary Layer Characteristics at Supersonic Speeds. CM 501 (UT/DRL 196), Contract NOrd-9195, Bur. Ord., Univ. Texas, Defense Res. Lab., Johns Hopkins Univ., Appl. Phys. Lab., Jan. 25, 1949.
- 24. Potter, J. L.: Friction Drag and Transition Reynolds Number on Bodies of Revolution at Supersonic Speeds. NAVORD Rep. 2150, U.S. Naval Ord. Lab., White Oak, Md., Aug. 20, 1951.
- 25. Young, George B. W., and Janssen, Earl: The Compressible Boundary Layer. Jour. Aero. Sci., vol. 19, no. 4, Apr. 1952, pp. 229-236, 288.
- 26. Rubesin, Morris W., Rumsey, Charles B., and Varga, Steven A.: A Summary of Available Knowledge Concerning Skin Friction and Heat Transfer and Its Application to the Design of High-Speed Missilés. NACA RM A51J25a, 1951.
- 27. Lees, Lester: The Stability of the Laminar Boundary Layer in a Compressible Fluid. NACA Rep. 876, 1947. (Supersedes NACA TN 1360.)
- 28. Eber, G. R.: Recent Investigation of Temperature Recovery and Heat Transmission on Cones and Cylinders in Axial Flow in the N.O.L. Aeroballistics Wind Tunnel. Jour. Aero. Sci., vol. 19, no. 1, Jan. 1952, pp. 1-6 and 14.
- 29. Chapman, Dean R.: An Analysis of Base Pressure at Supersonic Velocities and Comparison With Experiment. NACA Rep. 1051, 1951. (Supersedes NACA TN 2137.)
- 30. Schubauer, G. B.: Turbulence Measurements in the NACA 9-Inch Supersonic Wind Tunnel at Mach Number 1.9. Preliminary Rep. Ref. No. 6.3, Nat. Bur. Standards, Jan. 19, 1948.





- 31. Kurzweg, H. H.: Interrelationship Between Boundary Layer and Base Pressure. Jour. Aero. Sci., vol. 18, no. 11, Nov. 1951, pp. 743-748.
- 32. Bogdonoff, Seymour M.: A Preliminary Study of Reynolds Number Effects on Base Pressure at M = 2.95. Jour. Aero. Sci., vol. 19, no. 3, Mar. 1952, pp. 201-206.



UNCLASSIFIEU

Figure 1. - Drawing of models. All dimensions are in inches.

UNCLASSIFIED

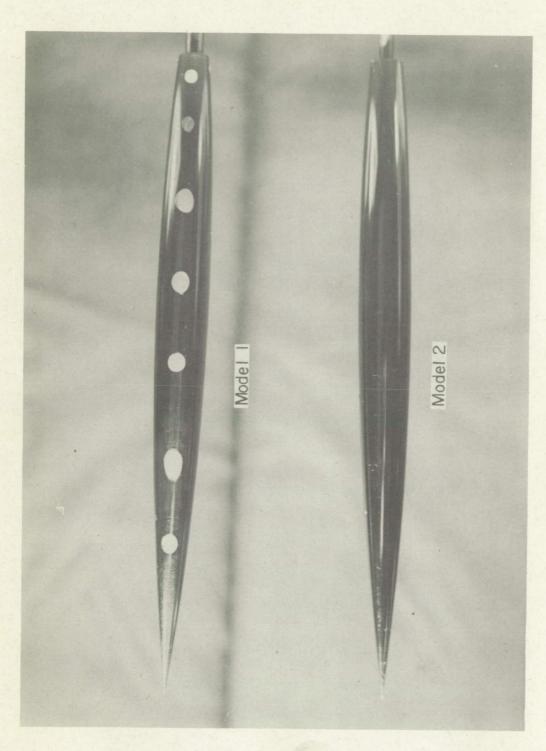
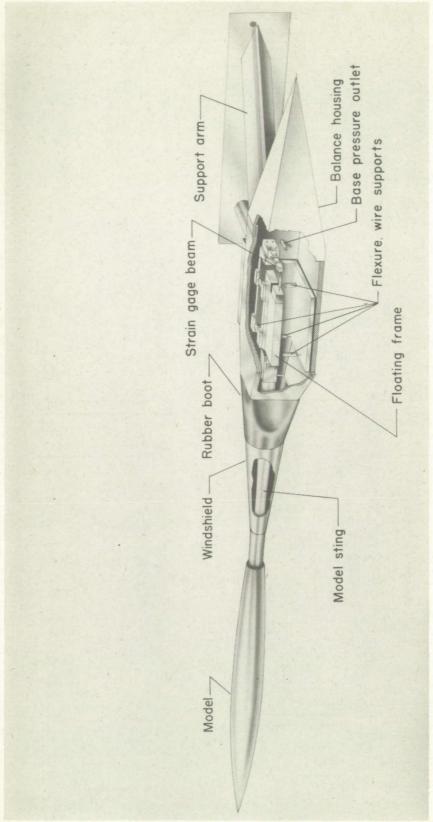


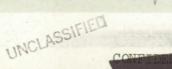
Figure 2. - Photographs of models 1 and 2.

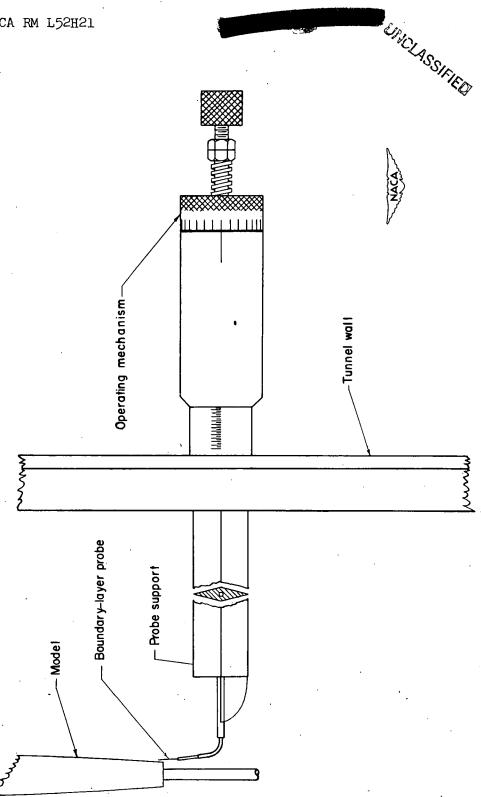
UNCLASSIFIED



1-76144

Figure 3. - Floating sting balance.

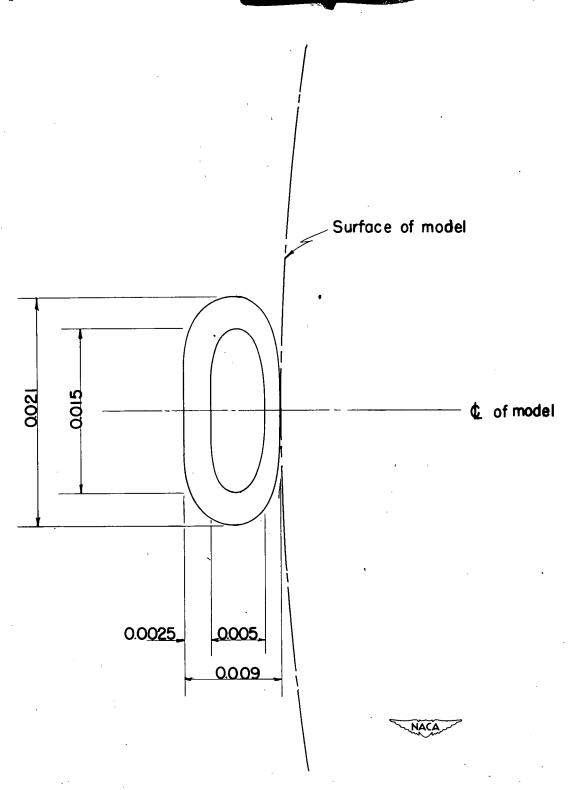




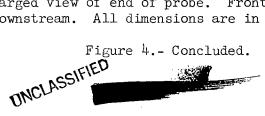
(a) Support and operating mechanism.

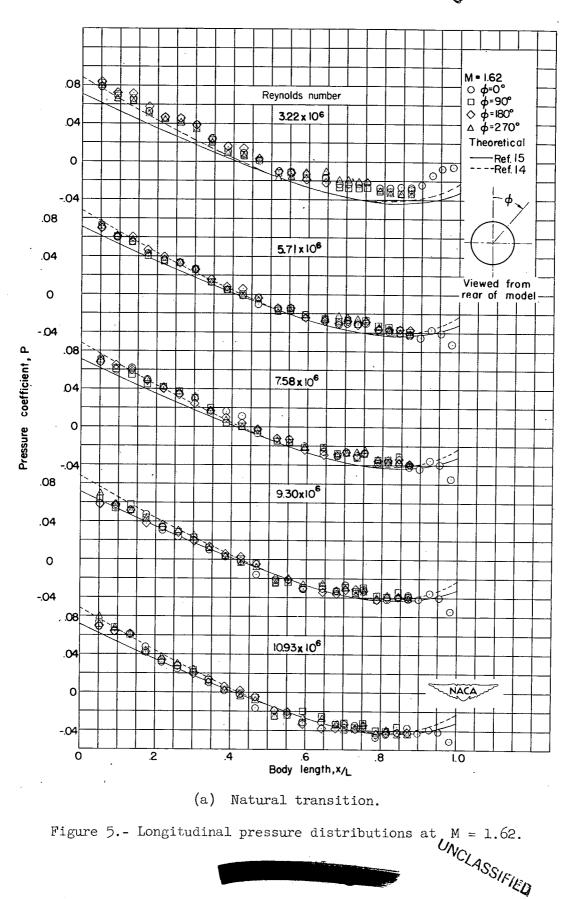
Figure 4. - Boundary-layer survey apparatus.



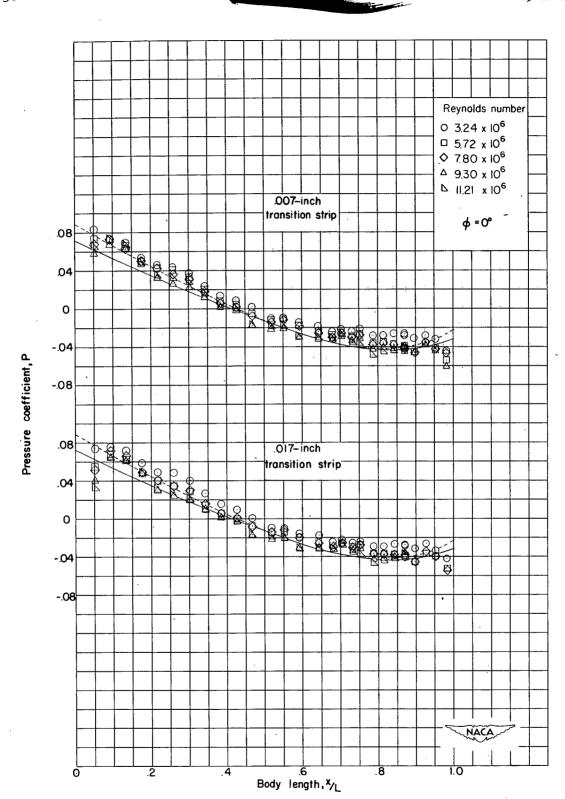


Enlarged view of end of probe. Front view looking (b) downstream. All dimensions are in inches.

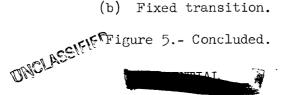


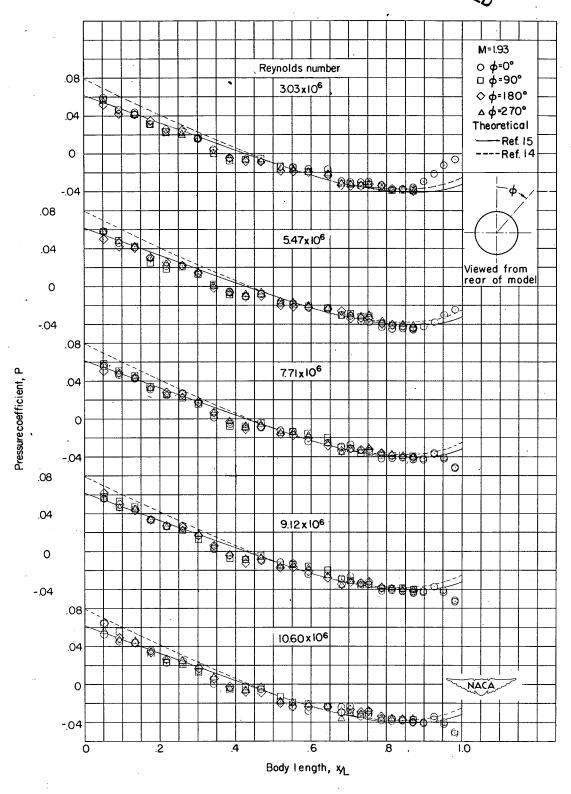






Fixed transition.



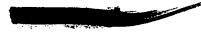


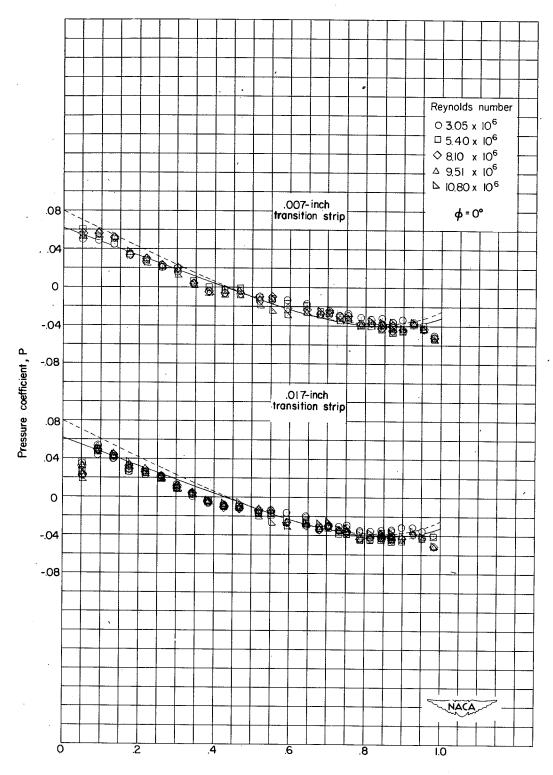
(a) Natural transition.

Figure 6.- Longitudinal pressure distributions at M = 1.93.



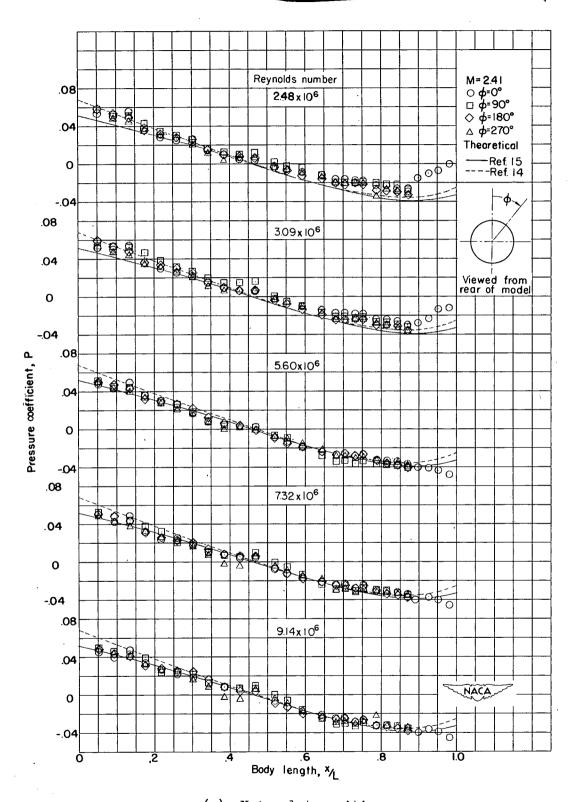
UNCLASSIE





Body length, x/L

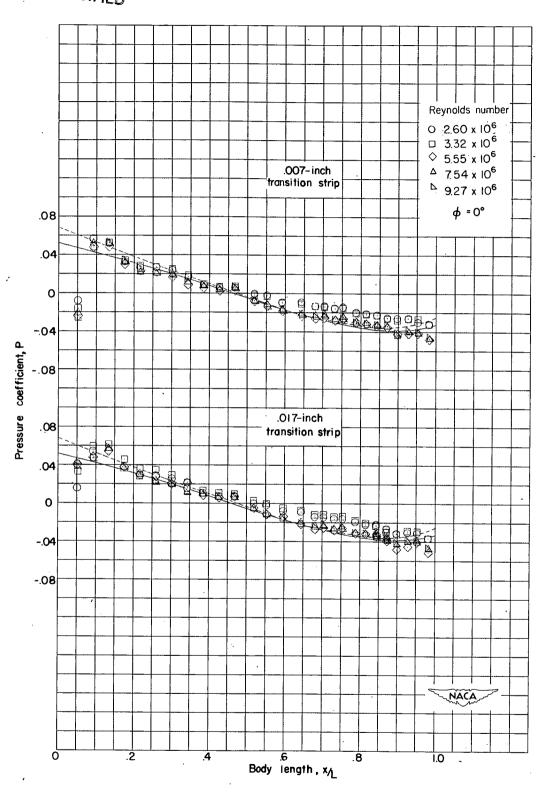
(b) Fixed transition.



(a) Natural transition.

Figure 7.- Longitudinal pressure distributions at M = 2.41.





(b) Fixed transition.

Figure 7.- Concluded.





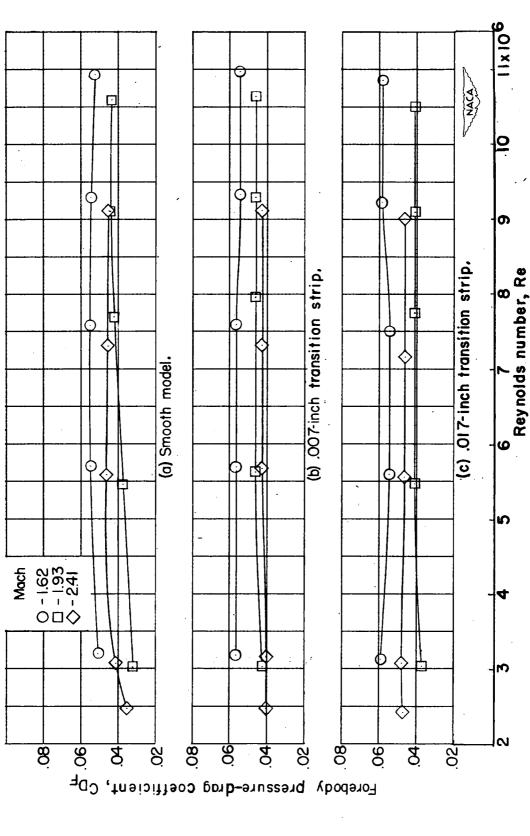


Figure 8.- Variation of forebody pressure-drag coefficient with Reynolds number

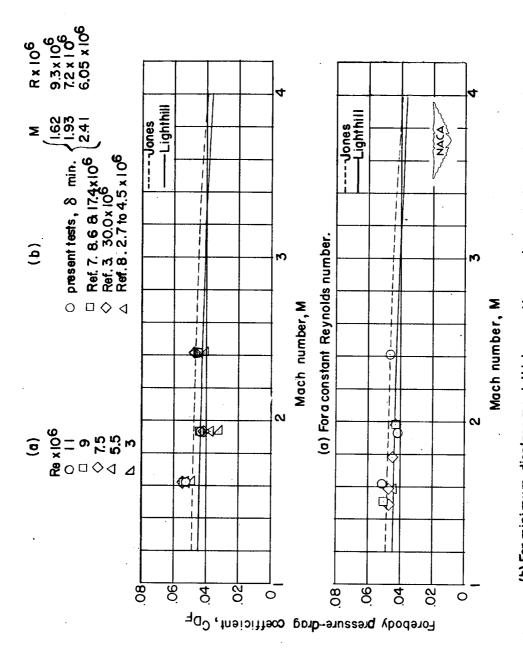


Figure 9.- Variation of forebody pressure-drag coefficient with Mach number. (b) For minimum displacement thickness at base and correlation with other data.

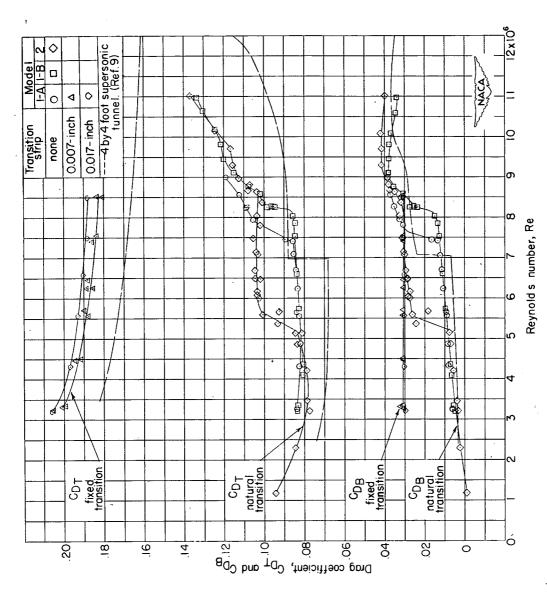


Figure 10. - Variation of total and base drag with Reynolds number for natural and fixed transition at M = 1.62.



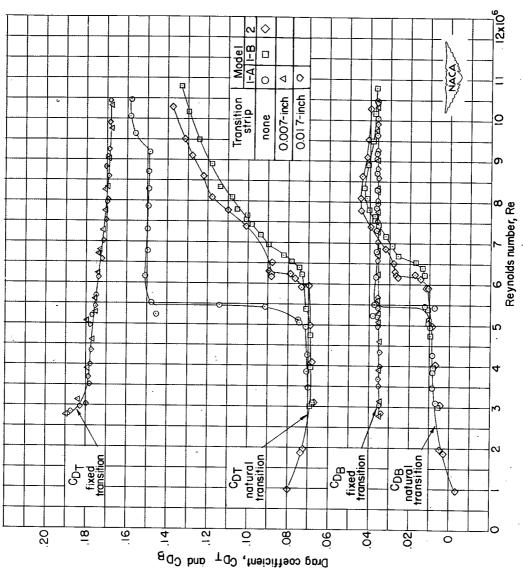


Figure 11.- Variation of total and base drag with Reynolds number for = 1.93.natural and fixed transition at M

Maintenie.

2:3

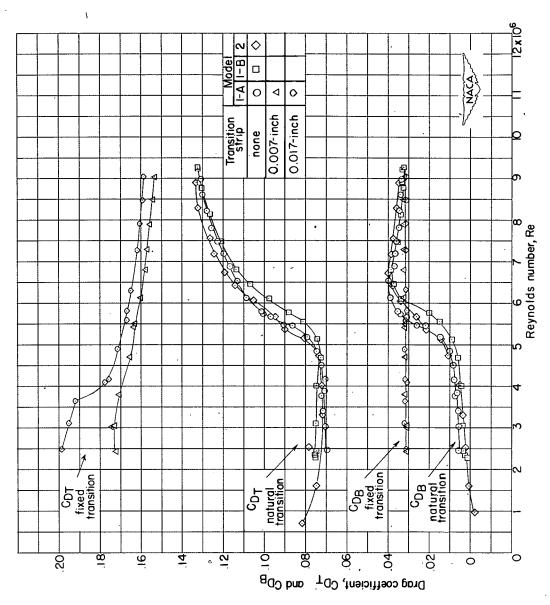
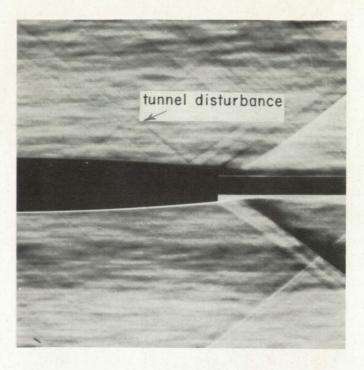
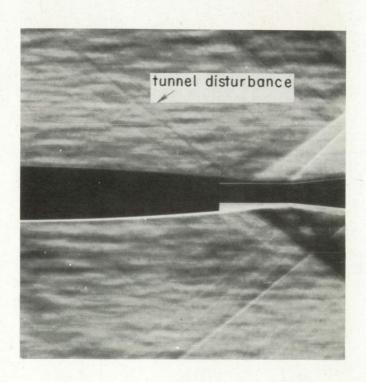


Figure 12. - Variation of total and base drag with Reynolds number for natural and fixed transition at M = 2.41.

CACLASSIFIED



(a) Model 1-B.



(b) Model 2.



Figure 13.- Position of weak tunnel disturbance at $\,\mathrm{M}=1.62\,\,\mathrm{with}\,$ respect to model test positions.



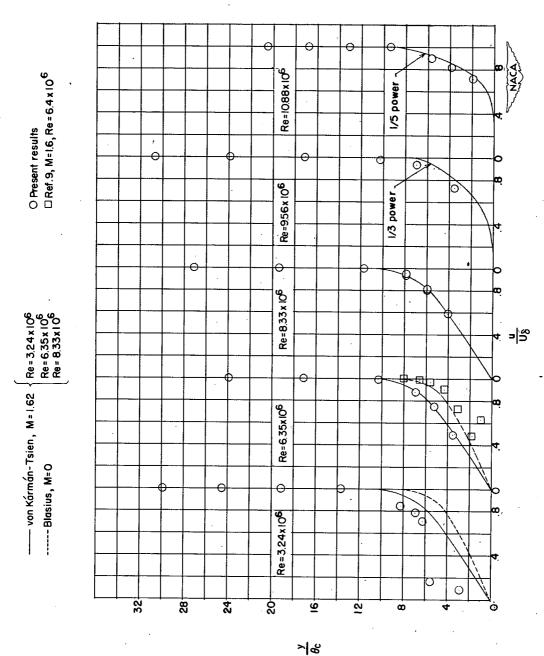


Figure 14.- Variation of nondimensional velocity profiles with Reynolds number at M=1.62.



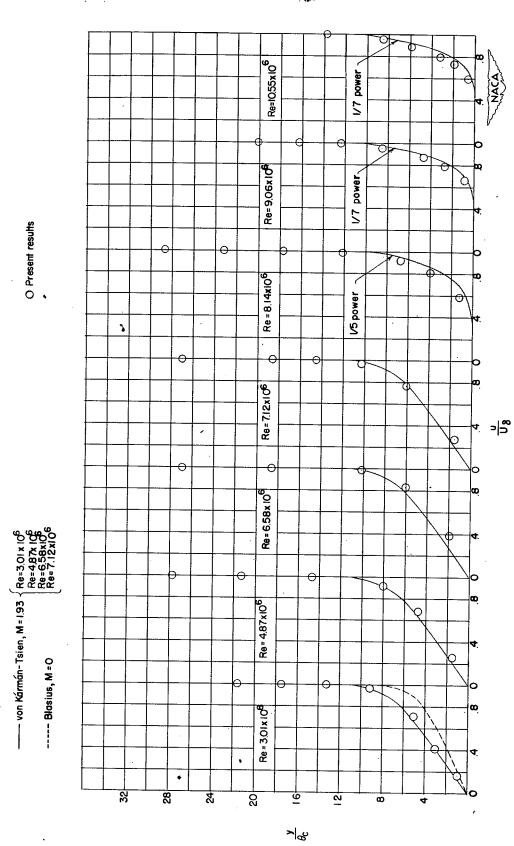
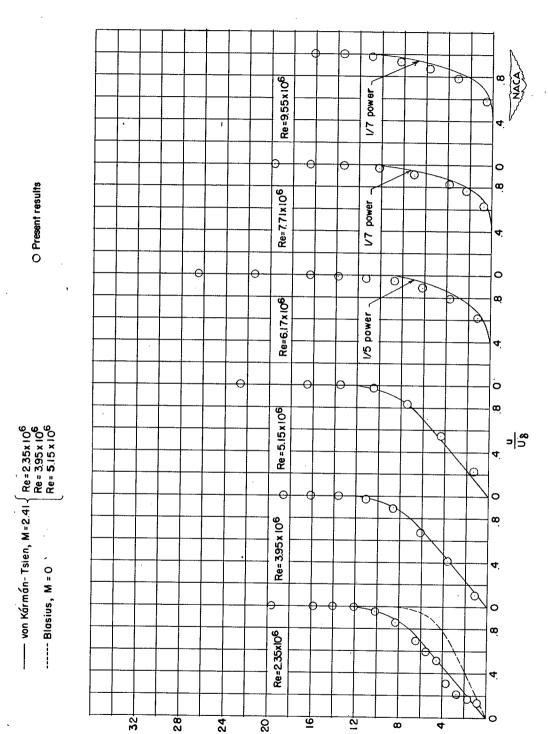


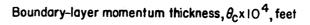
Figure 15.- Variation of nondimensional velocity profiles with = 1.93.Reynolds number at M





7/8

Figure 16. - Variation of nondimensional velocity profiles with Reynolds number at M = 2.41.



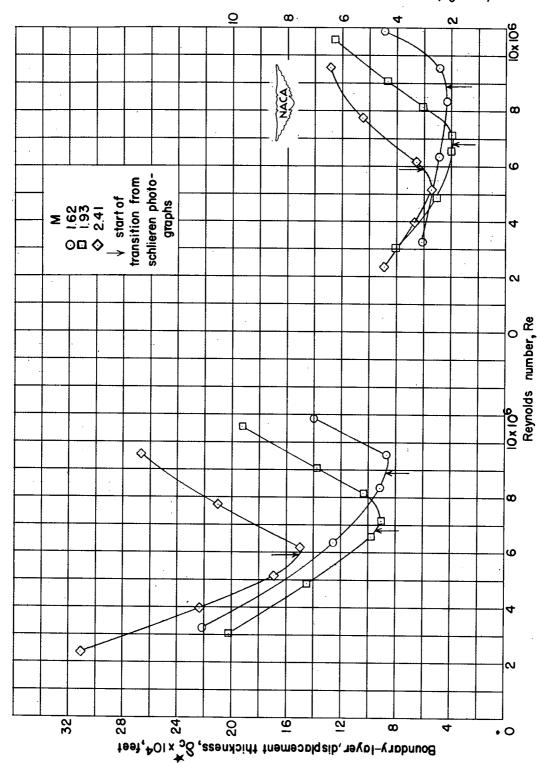
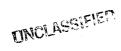
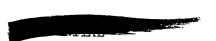
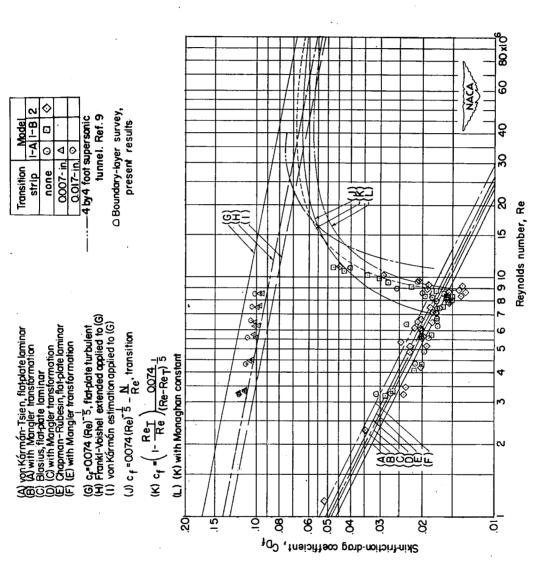


Figure 17.- Variation of displacement and momentum thickness with Reynolds number at all Mach numbers,





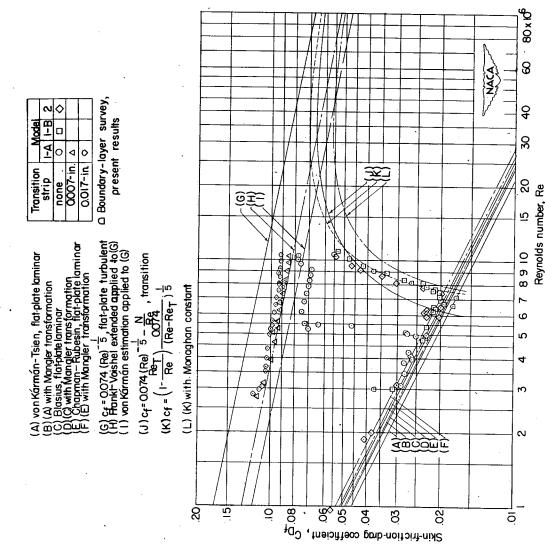




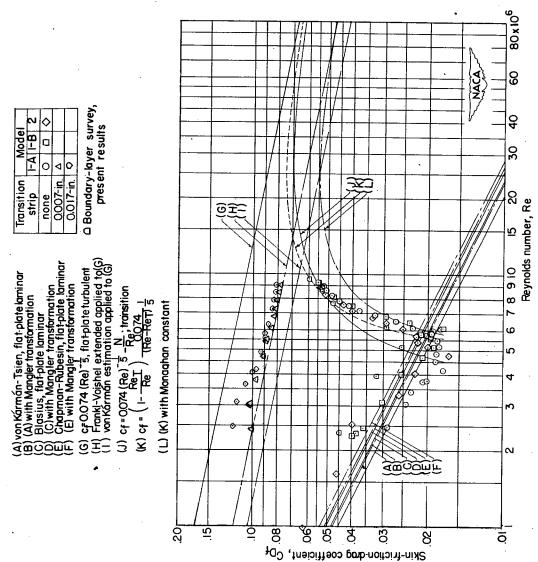
skin-friction-drag coefficient with Reynolds number at M = 1.62. Figure 18.- Variation of







skin-friction-drag coefficient with Reynolds M = 1.93.number at Figure 19.- Variation of



skin-friction-drag coefficient with Reynolds M = 2.41number at Figure 20. - Variation of

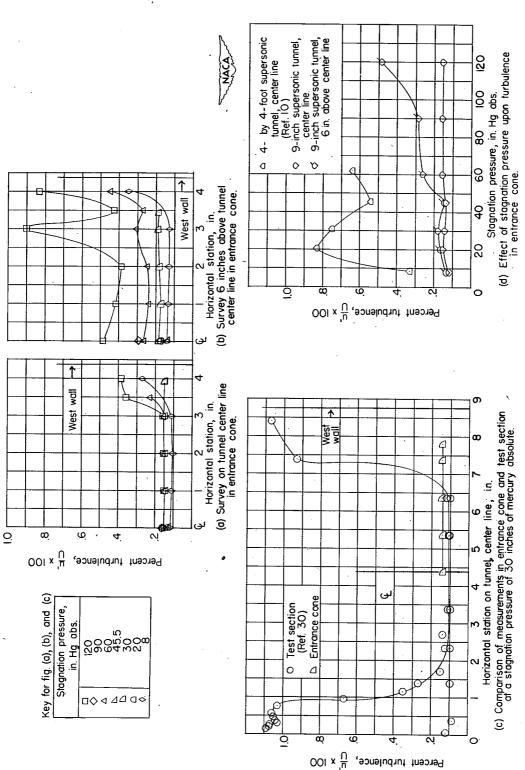


Figure 21. - Results of turbulence-level measurements in Langley 9-inch = 1.93.Σ supersonic tunnel at

TINCLASSIFIED

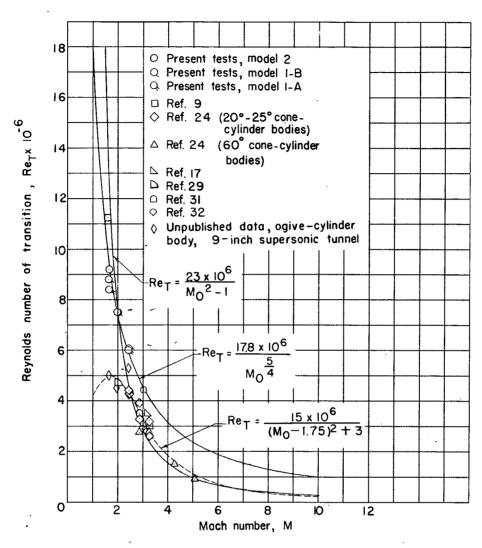


Figure 22. - Variation of Reynolds number of transition with Mach number for bodies of revolution.

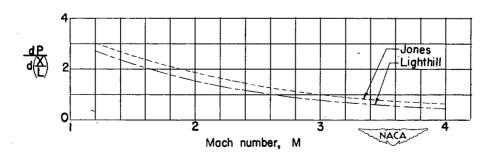
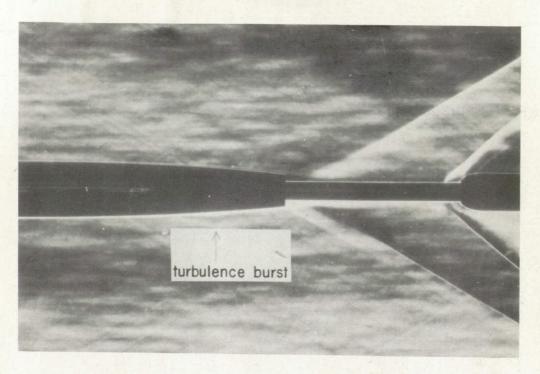
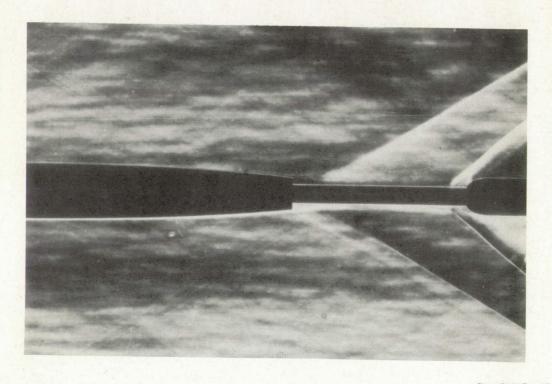


Figure 23.- Variation of pressure gradient at rear of RM-10 body with Mach number.





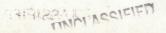
(a) With turbulence burst.



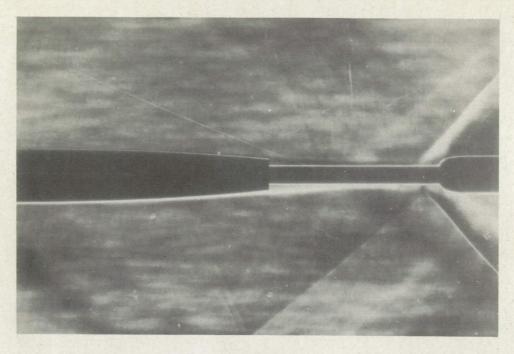
(b) Without turbulence burst.

L-76146

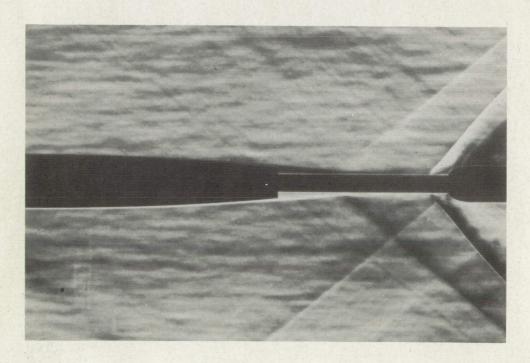
Figure 24. - Turbulence burst on model 1-B at M = 1.93, $R_e = 7.55 \times 10^6$.







(a) $R_e = 3.18 \times 10^6$.



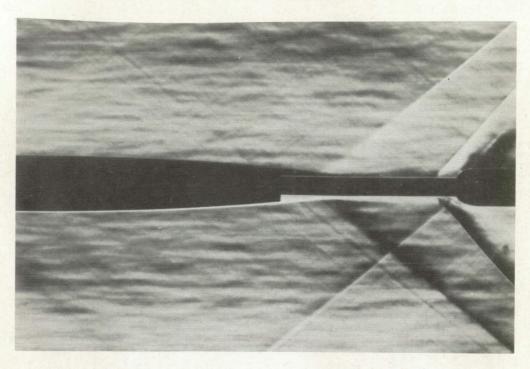
(b) $R_e = 6.29 \times 10^6$.

L-76147

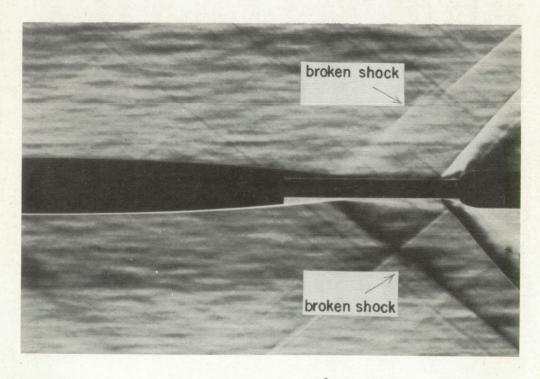
Figure 25.- Effect of varying Reynolds number upon the boundary layer, wake, and trailing-shock phenomena of model 1-B at M = 1.62.







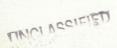
(c) $R_e = 8.07 \times 10^6$.

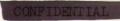


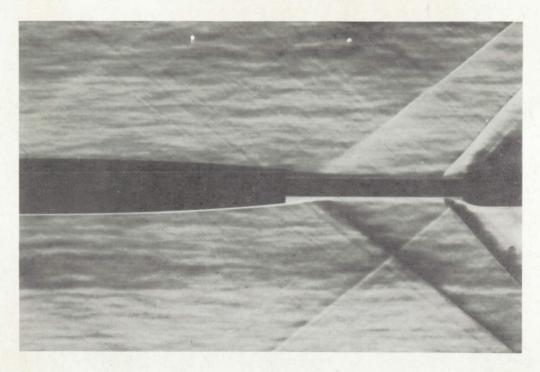
(d) $R_e = 8.07 \times 10^6$.

Figure 25.- Continued.

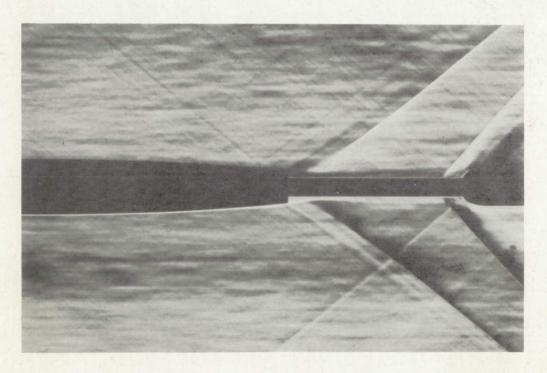
L-76148







(e) $R_e = 8.28 \times 10^6$.

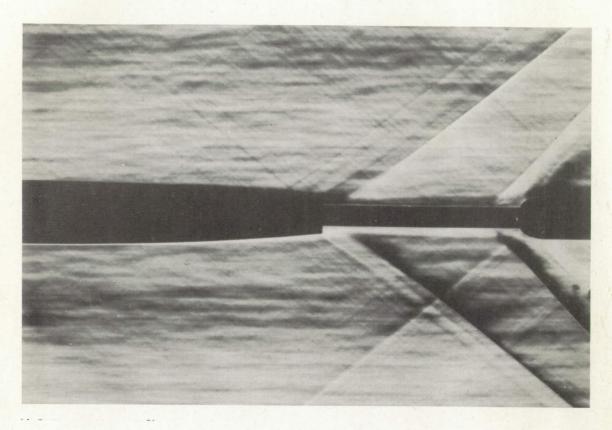


(f) $R_e = 9.61 \times 10^6$. Figure 25.- Continued.



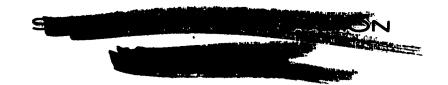
UNCI ASSIFIED

, full- winds Ci - volume in Pro-



(g) $R_e = 10.77 \times 10^6$. Figure 25.- Concluded.

NACA L-76150



UNCLASSIFIED

1184 . .